Molecular Crystals and Liquid Crystals
Publication details, including instructions for authors and subscription information:
http://www.tandfonline.com/loi/gmcl16

Order Parameter Distribution for the Electrophydrodynamic Mode of a Nematic Liquid Crystal

P. Andrew Penz [a]
[a] Scientific Research Staff, Ford Motor Company, Dearborn, Michigan
Version of record first published: 21 Mar 2007.

To cite this article: P. Andrew Penz (1971): Order Parameter Distribution for the Electrophydrodynamic Mode of a Nematic Liquid Crystal, Molecular Crystals and Liquid Crystals, 15:2, 141-160

To link to this article: http://dx.doi.org/10.1080/15421407108083231

Molecular Crystals and Liquid Crystals. 1971. Vol. 15, pp. 141–160

Printed in Great Britain

Order Parameter Distribution for the Electrohydrodynamic Mode of a Nematic Liquid Crystal†

P. ANDREW PENZ

Scientific Research Staff,
Ford Motor Company,
Dearborn, Michigan

Received October 23, 1970; *in revised form February* 12, 1970

Abstract—AC electric fields are known to induce a visible domain pattern in certain nematic liquid crystals. We have measured the focal length of the liquid crystal lens system responsible for this visibility. We have also measured the resistance change associated with this electrohydrodynamic mode. These results can be quantitatively interpreted in terms of the director's spatial distribution which is predicted by Helfrich's theory of conduction induced alignment.

1. Introduction

The effects of electric fields on liquid crystals have recently aroused considerable interest because of their applications in display devices[1] and because of attempts to explain them by the current description of mesomorphic liquids. We have studied the Williams domain pattern[2,3] observed in *p*-azoxyanisole, a nematic liquid crystal. The basic effect consists of the appearance of bright domain lines in a liquid crystal to which a sufficient voltage has been applied. While these domain lines are quasi-stationary for voltages near threshold, several observations have shown that there is fluid rotation spatially coherent with the lines.[4–9] In an earlier paper, we have demonstrated the focusing mechanism responsible for the visible domain lines.[6] Here we give a more detailed discussion of the focusing model and additional resistance measurements which support this model. The model is in close quantitative agreement with Helfrich's conduction-induced alignment theory.[10] A review of the early experiments using electric fields on nematic liquid crystals is given in an appendix.

† Presented at the Third International Liquid Crystal Conference in Berlin, August 24–28, 1970.

2. Experimental Procedure

We have used the customary experimental configuration with the PAA contained in a parallel plate capacitor having at least one transparent electrode. Prior to assembly the electrodes were wiped vigorously along a single direction to promote a uniform alignment of the order parameter $\vec{S}$.[11] An orthogonal coordinate system is defined by choosing the x axis along the rubbing direction. The z axis is defined by the direction of the sample thickness d which was fixed by Teflon spacers. The electric field was applied in the z direction by an audio frequency generator. In this coordinate system the domain lines and the vortices are oriented parallel to the y direction.

The PAA was purchased commercially and used without further purification. At 100 Hz and 130 °C, sample resistivities were in the 10^5–10^6 Ωm range, and the dielectric constant was approximately 6. Large increases in effective capacitance and resistance at lower frequencies indicated the presence of considerable ionic conduction, probably due to impurities. The addition of ionic impurities did not change the basic features of the domain pattern. The optical experiments were performed with a Leitz polarizing microscope in the transmission mode. A Leitz hot stage maintained the temperature in the PAA liquid crystal phase, 116 to 136 °C. The sample resistance and capacitance were measured by a standard audio frequency bridge. The sample temperature during the impedance measurements was regulated to 0.1 °C by a proportional temperature controller.

Figure 1 presents an idealized model which contains the basic experimental observations. The figure shows a cross section of the capacitor; the rubbing direction is horizontal; the microscope service is below and the observer is above the sample. The several stars indicate cross sections of the domain lines which run perpendicular to the page, the y direction. At voltages just above threshold we observe two sets of domain lines, both lying outside the liquid crystal. The positions of the lines are determined by making use of the limited depth of f cus inherent in optical microscopes at high magnification. The lines above the sample midplane are in focus at $(x, z) = ([n \pm \frac{1}{4}]\lambda_t, N'(\mathrm{V})r)$, and the bottom lines at $(x, z) = (n\lambda_t/2, -N(\mathrm{V})r)$, where n is an integer, $r = d/2$ and λ_t is the threshold wavelength in the x

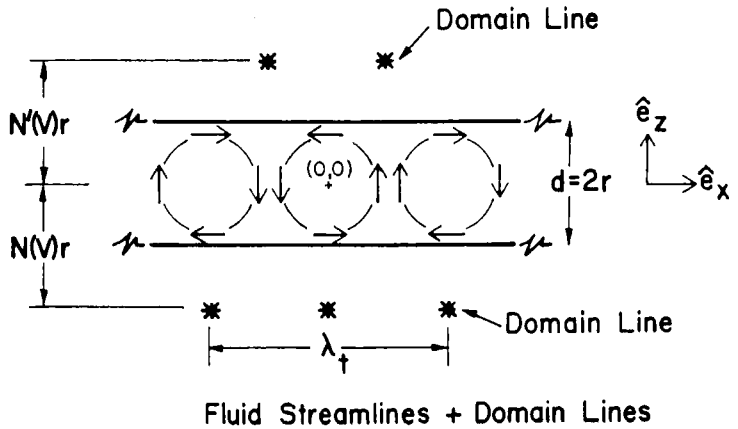

Figure 1. Idealized experimental observations. The figure is a schematic drawing of a capacitor cross section. The x direction is defined by the rubbing used to promote the director alignment. The driving electric field is applied in the z direction. The origin of the coordinate system is at (0, 0) and the capacitor plates are at $z = \pm d/2$. The streamlines inside the capacitor represents the fluid vortex pattern observed by tracer particle motion. The vorticity is antiparallel adjacent cells. The stars above and below the sample represent cross sections of the Williams domain lines. Both sets of domain lines have a separation in the x direction of $\lambda_t/2$. The upper domain lines appear at $z = N'(V)r$, the lower at $N(V)r$. The upper lines appear above the common flow pattern between the vortices. The lower domain lines appear below the centers of the vortices.

direction. N and N' are coefficients whose value is voltage dependent; this dependence will be described below. The model is idealized to the following extent. The height of the domain lines above regions of ascending flow tends to be less than the height of the lines above regions of descending flow. Thus $N'(V)r$ represents an average position of the top lines, and variations of up to 30% have been observed. To within experimental accuracy, all bottom lines lie at the distance $N(V)r$. The spacing between the bottom lines is observed to be $\lambda_t/2$ to within experimental error. The spacing between the top lines is better described experimentally by $(\frac{1}{2}+\Delta)\lambda_t$, $(\frac{1}{2}-\Delta)\lambda_t$, $(\frac{1}{2}+\Delta)\lambda_t$, etc., where $\Delta \sim 0.05$.

We find that the Williams domain pattern is accompanied by fluid rotation which is spatially correlated with the domain pattern. The roughly circular fluid motion is traced out by the motion of visible particles suspended in the liquid. Typical particle diameters are 5μm and may be easily resolved at $\times 100$ magnification. The stream lines lie in the x–z plane as indicated in the figure. The vortex lines

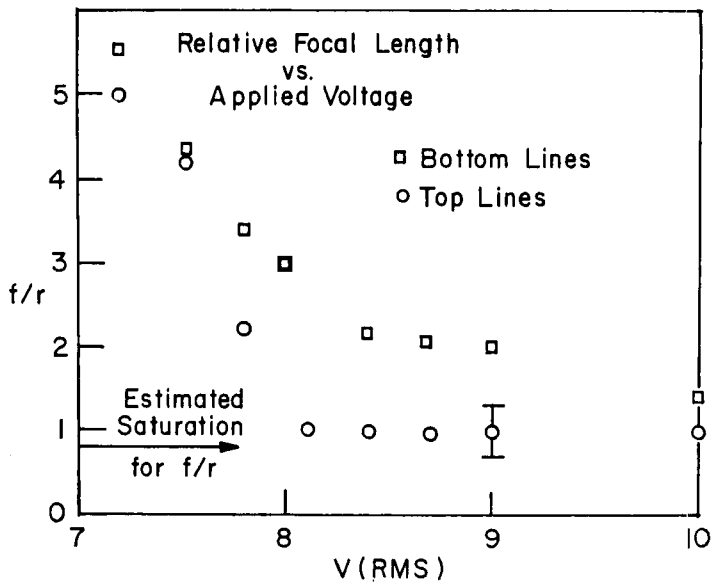

Figure 2. Relative focal length vs. applied voltage. The ordinate of the graph is the distance the domain line appears above (or below) the sample midplane divided by half the sample thickness: $f/r = N'$ (or N). The abscissa is the RMS voltage applied across the sample. The relative position of the top lines $N'(V)$ are given by the circles. The relative positions of the bottom lines are given by squares. The general tendency is for the line positions to decrease from a large value at threshold (near 7V) to a saturation value equal to half the sample thickness. The line labelled " Estimated Saturation " at $f/r = 0.8$ is the value predicted on the assumption that the saturation angle for the drumhead model is 45° and using the experimental value $rq = 1.8$.

lie along the y direction and are antiparallel in adjacent vortices. The observed particle orbits have steady-state diameters of approximately $\lambda_t/2$. Orbit periods at threshold range from several seconds for $d = 125$ μm to fractions of a second for $d = 38$ μm.

The observation of *bright* lines implies that light is being focused instead of scattered. The liquid crystal acts as a lattice of cylindrical lenses, producing real and virtual images of the microscope lamp source at voltage variable focal lengths $f = N'(V)r$ or $N(V)r$ respectively.

The coefficients N' and N are measures of the position of the domain lines above and below the sample midplane in units of half the sample thickness r. They are approximately equal and depend on voltage. Figure 2 shows a plot of N' (circles) and N (squares) as a

function of the RMS voltage applied. The ordinate in Fig. 2 is labeled f/r. Just above threshold, typical values of the relative positions are 5. There is a decrease with increasing voltage, saturating at approximately unity a few volts above threshold. The somewhat different behavior of N' and N with voltage is thought to be a real experimental effect, but the general similarity is the significant feature. As the voltage is raised further, the domain positions become increasingly dynamic in the x–y plane. It is this turbulence

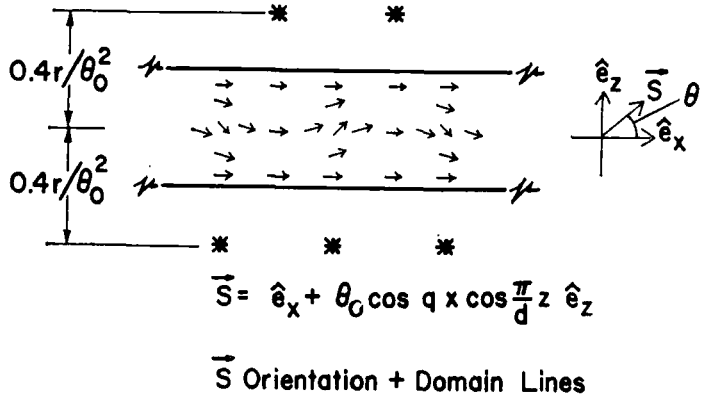

Figure 3. Drumhead Model for the Director $\vec{S}$. The figure shows the spatial variation of S which is consistent with the experimental measurements of focal length and resistance. The cross section of the capacitor is to be interpreted as identical to Fig. 1. The director is represented by small arrows and is drawn to fit the $\cos qx \cos \pi z/d$ drumhead pattern. The origin of the coordinate system is at the center of the center pattern. Comparison with Fig. 1 shows that the maximum tipping angle is at the center of the vortex motion. Using the known indices of refraction of PAA, the focal length for this model is $0.4\ r/\theta_0^2$.

which gave rise to the term dynamic scattering mode (DSM).[1] It is difficult to precisely determine the N and N' values of these rapidly moving lines, but they definitely remain at approximately unity at higher voltages. In this paper we consider only the relatively stable Williams domain pattern.

Since one of the most characteristic qualities of a liquid crystal is its birefringence, it might be expected that a spatial variation of S could produce focusing. Figure 3 illustrates a distribution of the director which is consistent with the experimental observations. The director is described by the formula $\vec{S} = \hat{e}_x \cos\theta + \hat{e}_z \sin\theta$, where

θ is the angle $\vec{S}$ makes the $\vec{x}$ axis. If $\theta = \theta_0 \cos qx \cos \pi z/d$ and if θ_0 is small:

$$\vec{S} = \hat{e}_x + \theta_0 \cos qx \cos \pi z/d \, \hat{e}_z \tag{1}$$

where $\hat{e}_x$ and $\hat{e}_z$ are appropriate unit vectors, θ_0 is the amplitude of the distortion and $q = 2\pi/\lambda$. The pattern specified by Eq. (1) is shown in Fig. 3. The spatial variation of the z component of $\vec{S}$ is similar to the first mode of a rectangular drumhead and thus will be referred to as the drumhead model. We now show that Eq. (1) predicts the correct qualitative optical focusing.

Since the spatial distribution of θ has been assumed, the spatial distribution of the z component of the index of refraction can be found from the identity $n_z = n_e \cos^2 \theta + n_o \sin^2 \theta$ where n_o (ordinary ray) and n_e (extraordinary ray) are the indices of refraction perpendicular and parallel to S respectively. Using Eq. (1) it follows that:

$$n_z = n_e + (n_o - n_e)\theta_0^2 \cos^2 qx \cos^2 \pi z/d.$$

This formula is valid only for light polarized in the x direction. For polarization in the y direction, there is no variation of the index of refraction from n_0. The optical path length is $L = \int n_z \, dz$. It is straightforward to calculate the focal lengths associated with such a distribution since L is a quadratic function of x near $x = 0$ or $\pm d/2$. This is just the dependence found for a thin lens, and so by analogy: $-1/f = \partial^2 L/\partial x^2$ at $x = 0$ or $\pm d/2$. Performing this integration and differentiation yields:

$$f = \pm[(n_e - n_o)\theta_0^2 q^2 d]^{-1} \tag{2}$$

where the plus sign refers to $x = \pm \lambda_t/4$ and the minus sign to $x = 0$. Since n_o is less than n_e,[12] the distribution in Eq. (1) predicts the correct qualitative focusing. This can be seen by the following physical argument. At $x = \pm \lambda_t/4$, the director is parallel to x everywhere and only n_e will enter the formula for L. Since n_e is a maximum, L will be maximum; the focusing will be converging, producing a real image. By the same reasoning, the optical path will be shortest at $x = 0$, and a diverging lens will produce an imaginary image there. Finally since n_e and n_o are known, and q can be measured, the data in Fig. 2 can be used to compute θ_0 as a function of applied voltage. This analysis will be presented after discussion of the resistance data.

3. Resistance Measurement

Since the application of an audio frequency electric field to a liquid crystal produces variations in the optical frequency electric susceptibility, it is natural to look for changes in the audio frequency susceptibility, i.e. the resistance and capacitance. Unfortunately the experiment seems to be practically limited to a two probe technique. The current probes are the capacitor plates. Separate voltage probes would require insertion of wires into the liquid. The fact that fluid flow is fundamental to the effect rules out such voltage probes because of their unknown effect on the fluid flow. It is conceivable that such leads would fundamentally alter the measurements. Consequently one is forced to measure the bulk impedances of the liquid crystal in series with the contact impedances at the electrodes. In order to compare the impedance experiment with the drumhead model it is necessary to insure that contact impedances are small and not field sensitive.

We have found experimental evidence that suggests that electrode phenomena dominate the measured impedances of our material at very low frequencies. Typically for frequencies below 100 Hz, the resistance of the sample *increases* with increasing voltage. Increases of as much as 10% have been observed upon changing from 0 to 20 V at 100 Hz. There is a definite dispersive character to both the resistance and the capacitance of the PAA sandwich cells. Generally, both the resistance and the capacitance increase with decreasing frequency. The DC resistance can be as much as a factor of 10 larger than the resistance at 100 Hz. The low frequency capacitance can rise a similar order of magnitude. This behavior persists into the isotropic state. It is experimentally observed that for frequencies above 100 Hz where there is little or no dispersion, the resistance of the sample is voltage *independent* to the order of 1% from 0 to 5 V.

There seems to be no connection between this very low frequency, dispersive, non-ohmic behavior and the domain pattern. Since this paper is concerned with the domain question, we have chosen to work in the frequency range above 100 Hz where changes in the sample resistance can be directly correlated with the domains. It is expedient to do this because the very low frequency effects probably involve electrode effects, usually a very difficult problem. Electro-

chemical polarization due to charge transfer and mass transfer are well known and are traditionally eliminated by working at sufficiently high frequencies (1 kHz–10 kHz). Electrophoresis could also have an effect at low frequencies. While these effects seem to be a reasonable explanation on cursory examination, we do not intend to rule out other explanations. Certainly these effects should be considered, however, in analysis of a DC or very low frequency impedance experiments.

There is another frequency dependence associated with the experiment, and it can be directly correlated with the domain pattern. There is an upper frequency limit on domain formation, typically 10 kHz. For larger frequencies, the threshold voltage increases rapidly with frequency. The functional form resembles $\exp[f2\pi RC]$ where C is the capacitance and R the resistance. This frequency dependence of the threshold voltage suggests that the mechanism responsible for the domains depends on space charge. The frequency of the driving voltage must remain below the space charge relaxation frequency $1/2\pi RC$ in order for the domain effect to be non-dispersive. It should be noted that we have not observed the chevron pattern,[9] possibly because of the high conductivity of our samples.

The sample impedance was measured using a standard audio frequency bridge. The output of the bridge was phase sensitively detected and plotted as a function of the voltage which the bridge circuit produced across the sample. A typical plot of experimental data is shown in Fig. 4 for the bridge output in phase with the drive current. Basic circuit analysis shows that this output voltage is $V\Delta R/R$, where R is the sample resistance and ΔR is the change in resistance. While Fig. 4 represents a convenient method for data accumulation, it does not lend itself to easy interpretation. The difficulty is that V, the independent variable, is changing on both the ordinate and the abscissa. To obtain $\Delta R/R$, the ordinate must be divided by V. This fact must be kept firmly in mind when interpreting the two regions of Fig. 4. Since the bridge output is zero below 5 V, the resistance is independent of voltage, indicating Ohmic conduction. At threshold the bridge output abruptly begins to change, indicating a decrease in the sample resistance. The linear region above 5 V indicates that the resistance saturates at a 10% lower value a few volts above threshold. Similar resistance changes

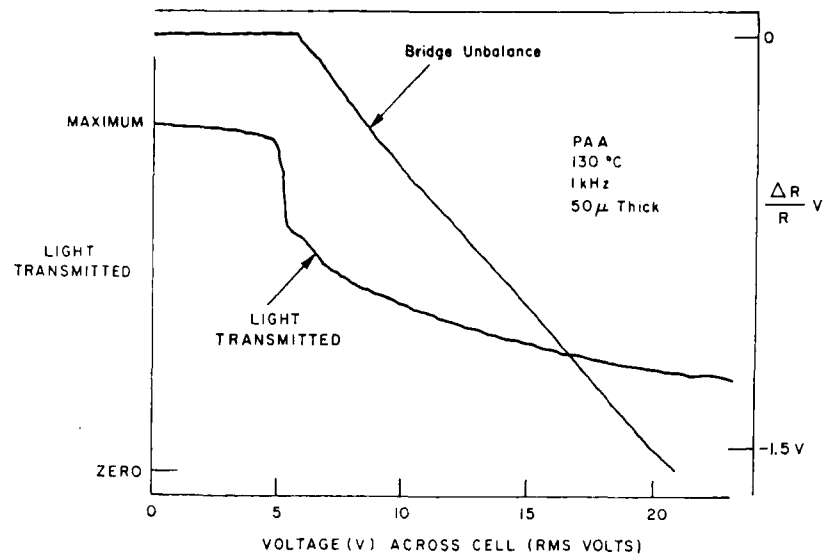

Figure 4. Resistance and Scattering Measurements. The figure presents the output of an audio frequency bridge as a function of the RMS voltage applied at 1k Hz. The bridge output is proportional to $V\,\Delta R/R$. The graph is constant below threshold, indicating ohmic conduction in the bulk liquid crystal. Near threshold the bridge output changes, indicating a decrease in sample resistance. Reduction of this experimental data indicates that the resistance decrease saturates so that the net change is a 10% decrease in resistance a few volts above threshold. To within the accuracy of the measurement, no capacitive change was seen. The figure also shows a measurement of the light transmitted through the liquid crystal, reflected off a mirror electrode and passed back through the sample. The transmission decreases sharply at threshold, as first noted by Williams.

have been observed by others.[13,14,15] Within the experimental uncertainty of 1%, we could not definitely identify a change in the capacitance.

Also plotted in Fig. 4 is the light transmitted through the cell and reflected off an aluminum mirror back through the cell.[2] It can be seen that the resistance change begins in the same voltage region where the optical properties change.

These resistance changes can be interpreted in terms of the drum-head model for the order parameter shown in Fig. 3. The argument proceeds in a manner similar to the focal length calculation. The resistivity component in the z direction is $\rho_z = \rho_\perp \cos^2\theta + \rho_\parallel \sin^2\theta$

where $\rho_\perp$ and $\rho_\parallel$ are the resistivities perpendicular and parallel to the director. Using the distribution given by Eq. (1),

$$\rho_z = \rho_\perp + (\rho_\parallel - \rho_\perp)\theta_0^2 \cos^2 qx \cos^2 \pi z/d,$$

in the approximation $\theta_0 \ll \pi$. The resistivity may then be averaged in the x and z directions giving:

$$\frac{\bar{\rho}_z - \rho_\perp}{\rho_\perp} = \frac{\rho_\parallel - \rho_\perp}{\rho_\perp}\frac{\theta^2}{4} = \frac{\Delta R}{R_0} \tag{3}$$

where $\bar{\rho}_z$ is the average resistivity and R_0 is the zero field resistance. Since for PAA $\rho_\parallel = (2/3)\rho_\perp$,[16] the drumhead model predicts that the resistance of the sample must decrease as θ_0 becomes finite above threshold. Just such behavior is depicted in Fig. 4. That the drumhead model predicts such a result is obvious when one remembers that $\theta_0 = 0$ means the director everywhere parallel to the capacitor plate. Since the resistivity perpendicular to the molecule is a maximum, any tipping of the director out of the x direction will produce a lower resistance. Note that the predicted change is independent of the pattern wavelength λ.

Equation (3) can be used to compute the tipping amplitude θ_0 as a function of voltage from the resistance data. This is shown in Fig. 5, along with similar but *independent* data from the focal length measurements. The tipping amplitude rises steeply to about 20° at half a volt above threshold and exhibits saturation at higher voltages. This general behavior is shown for three independent measurements, the resistance change, the focal length of the virtual image and the focal length of the real image. The agreement at higher voltages is only fair, but the general variations of focal lengths and resistance with field can be simultaneously explained by the drumhead model. The real and imaginary focal lengths do not yield the same tipping angle for the same voltage. This may have something to do with the fact that the real focal length involves liquid moving predominantly at the outside of the vortex. The liquid more to the center of the vortex produces the imaginary image. Surface and/or gravitational effects could produce differences. The fact that a capacitance change was not observed is consistent with this model since the anisotropy of ϵ is small $\epsilon_\perp/\epsilon_\parallel = 1.04$. While it is clear that θ_0 saturates at higher voltages, the true saturation value is not readily apparent from Fig. 5. The data has been computed

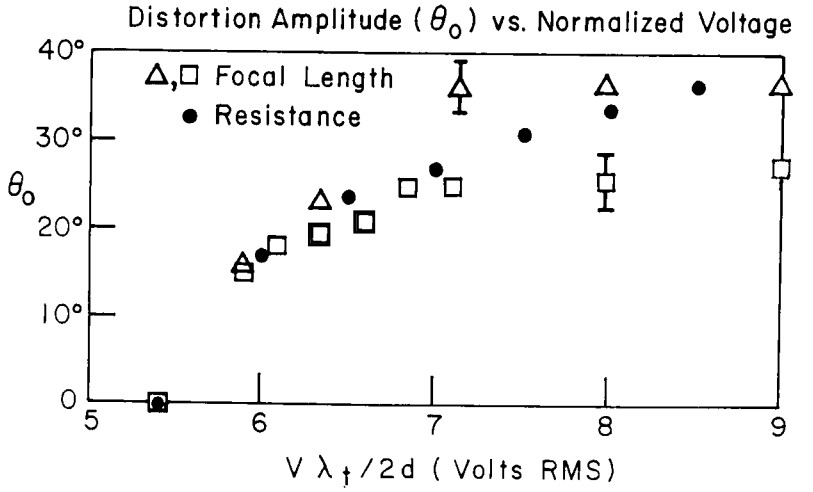

Figure 5. Distortion amplitude vs. normalized voltage. The distortion amplitude θ_0 has been calculated on the basis of the drumhead model from resistance and focal length data. The resistance data points are the closed circles. The imaginary focal lengths yield the angles plotted as squares. The real focal lengths implied the data in triangles. The general pattern from all three measurements is for θ_0 to increase sharply from its value of zero at threshold. θ_0 saturates at higher voltages at a value between 30 and 40°. It should be remembered that the figure was plotted from data reduced using a small angle approximation for θ_0. Thus the figure presents a consistent underestimate of the true distortion amplitude at higher voltages.

using the approximation $\sin\theta_0 = \theta_0$ which slightly overestimates $\sin\theta_0$ at $\theta_0 \sim 45°$ (for $\sin\theta_0 = 0.7$ radians, $\theta_0 = 0.8$ radians $= 45°$). Thus the saturation angle is *larger* than the values shown in Fig. 5. It is possible to improve the estimate of the saturation angle by replacing θ_0^2 in Eq. (2) by $\sin^2\theta_0$. Using $\theta_0 = 45°$, one predicts a saturation focal length of $0.8r$ which is within experimental error of the measured value of $1.0r$ (see Fig. 2). Thus the measured saturation value of θ_0 is in the neighborhood of 45°.

4. Threshold Voltage and Blocking Electrodes

It has been reported earlier that the threshold voltage V_t for domain formation is insensitive to thickness.[6,14,15] This feature is shown in Fig. 6, a log–log plot of V_t vs d. Clearly there is no large variation of V_t with d. The uncertainty at 1000μ is indicative of a

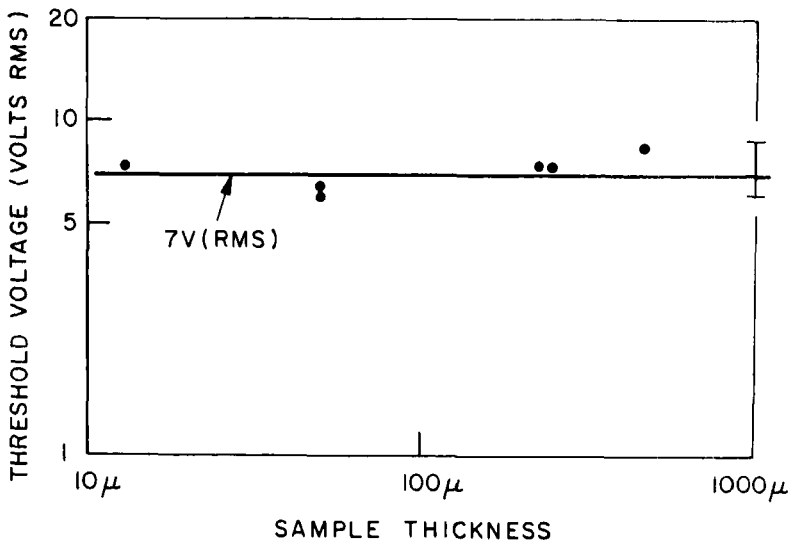

Figure 6. Threshold voltage vs. sample thickness. A log–log plot of threshold voltage vs. sample thickness is presented. It can be seen that V_t is not sensitive to d and lies close to the 7 V RMS magnitude. The large error bar at 1000μ indicates a very gradual turn-on of the pattern and a consequent uncertainty in the measurement for thick samples.

very gradual turn of the domain formation, making the determination of V_t difficult. We have found that the normalized voltage $V_t\lambda_t/2d$ is even less sample dependent, having a value of 5.5 ± 0.2 V RMS at 130 °C for a limited number of samples.[7] Deliberate doping of the samples with sufficient $N(CH_3)_3Cl$ and NaI to raise the conductivity an order of magnitude produced no noticeable change in V_t.

It is possible to observe the domain pattern using purely capacitive coupling. Thin sheets of mica over both electrodes were used to isolate the liquid crystal from sources of real charge. The sample still exhibited strong optical effects under AC excitation. The net voltage across the liquid at threshold remained in the 5–7 V range even with the mica sheets.

5. Theory

The basic coupling mechanism between the electric field and fluid motion does not appear to be a dielectric interaction. For PAA

$\epsilon_\perp > \epsilon_\parallel$ where $\epsilon_\perp$ is the dielectric constant perpendicular to the director and $\epsilon_\parallel$ is the parallel component.[17] Such an anisotropy should reinforce the tendency of the director to remain in the x–y plane of the capacitor and could not by itself lead to fluid motion. On the other hand, any net charge per unit volume, Σ, will couple to the electric field E with the body force ΣE which may in turn cause fluid motion. There are two competing theories for the origin of the space charge Σ, and we here review them briefly.

Recently there has been active interest in the space charge limited (S.C.L.) conduction in liquids as a mechanism for producing fluid motion.[18] The problem is formulated by consideration of unipolar current injection J into an insulator characterized by a mobility μ and dielectric constant ϵ. Solution of Poisson's equation, under the assumption of no fluid motion, gives $\Sigma = (\epsilon\epsilon_0 J/2\mu)^{1/2}(z+r)^{-1/2}$ where the current is being injected in the z direction as indicated by Fig. 1; ϵ_0 is the permittivity of free space. Rationalized MKS units are used throughout. The resultant electric field distribution is:

$$E_z = [2J(z+r)/\mu\epsilon\epsilon_0]^{1/2}. \tag{4}$$

Such a space charge distribution has the possibility for instability if the medium is a liquid. Using standard hydrodynamic theory with electrostatic coupling, Schneider and Watson[19] have shown that a hydrodynamic instability is to be expected at a voltage V_0:

$$V_0 \approx 100\,\frac{\mu\eta}{\epsilon\epsilon_0}. \tag{5}$$

While the calculation required numerical solution, V_0 can be derived from the physically sensible comparison of the electrostatic force with the viscous force. When this electrohydrodynamic Reynold's number reaches the typical value of 100, some fluid flow instability is to be expected. Equation (5) is the result of just such a physical model. Watson, Schneider and Till[20] have shown quantitative agreement between Eq. (5) and experiments on a silicone fluid. Clearly this mechanism requires none of the anisotropic properties of the liquid crystal phase. A straightforward estimate of V_0 to compare this mechanism with the threshold voltage for domain formation in PAA requires a knowledge of μ and η. An average viscosity for PAA is 5×10^{-3} kg/ms.[21] The ion mobility is calculated from our experiments

from the *assumption* that the ion velocity is the same as the fluid velocity, which is probably an underestimate.[18] The fluid velocity at a voltage of six volts was computed from the $\frac{1}{3}$ second traverse time for a piece of dust in a 50μ sample. The consequent mobility is 1.2×10^{-9} m²/Vs. An estimate of V_0 is 12 V. Thus the turn-on voltage for the injected space charge mechanism is close to the observed threshold voltage. Several other experimental details make the mechanism seem unlikely in the AC driven liquid crystal phase.

The first problem with the unipolar space charge injection mechanism is that at AC there is no evidence for the non-ohmic I–V characteristic predicted by Eq. (4). Our experiments have shown that below threshold the liquid crystal conduction is ohmic and that well above threshold the sample is again ohmic but with a 10% smaller resistance. Strong evidence for the lack of a SCL current in our samples arises from the consideration of the assumption made in deriving Eq. (4) that the medium was originally insulating. Our samples have a definite ohmic conduction, presumably by impurity ions of a density n_i. The resistivity associated with these ions is $(n_i e\mu)^{-1}$. The resistivity associated with Eq. (4) is $E/J = 2d/E\mu\epsilon\epsilon_0$. Clearly the SCL limited current will dominate the ohmic current when the ratio of the ohmic to the SCL resistivity becomes greater than unity. This reasoning yields an estimate for the voltage at which a changeover is expected:[22]

$$V_{SCL} = \frac{n_i e}{\epsilon\epsilon_0} d^2. \tag{6}$$

Note that this is the voltage which would be produced by completely sweeping n_i positive ions to one electrode and n_i negative ions to the other electrode.

In order to estimate V_{SCL}, an estimate of n_i is necessary. Since $\rho = (n_i e\mu)^{-1}$, $\rho \sim 10^6\,\Omega$ m and $\mu \sim 1.2 \times 10^{-9}$ m²/Vs, n_i can be estimated to be 10^{22} carriers/m³ (10^{16} carriers/cm³). Another estimate of n_i can be obtained from the relaxation frequency of the electrochemical polarization. If we assume that this relaxation frequency is diffusion limited and use the known diffusion coefficient of 10^{-9} m²/s,[23] a carrier density of 10^{24} m^{-3}(10^{+18} cm^{-3}) is obtained. Using the more conservative estimate of 10^{22} and a 50μ sample thickness, one

estimates $V_{SCL} = 10^5$ V. In the experimental voltage range of 0–100 V, one therefore expects that the current is primarily determined by ohmic conduction. Another argument against the SCL mechanism is that the associated relaxation time should be the order of magnitude of the time for a carrier to cross the sample: $\tau \sim$ seconds. This is much longer than the observed relaxation times: $\tau = RC \sim$ milliseconds. Finally, the SCL mechanism only predicts a fluid motion; a focusing mechanism has yet to be described.

These estimates demonstrate that SCL currents are not responsible for the fluid motion under the experimental conditions reported here, i.e. AC driving fields in the liquid crystal phase. At DC, however, there is the possibility of polarization of the impurity carriers. We have already demonstrated that such polarization is important below 100 Hz. Since the impurity ions are gathered at the electrodes, the bulk ohmic resistivity is increased. The estimate of V_{SCL} would then decrease, perhaps enough for the SCL mechanism to become important. That this may be the case has been shown by the observation of fluid motion in the isotropic phase.[8] Also the observed optical patterns in the liquid crystal phase seem to be different from AC[7] and DC[6] driving voltages.

Carr[24] has proposed a second mechanism for the generation of space charge which involves impurity ions and the anisotropic conductivity of the liquid crystal phase. Helfrich[10] constructed a theory based on these factors and showed that they can lead to an electrohydrodynamic instability at a threshold voltage. Once again the details of the theory are quite involved, but the basic physical ideas are straightforward. The technique is to consider the stability of a periodic fluctuation in the director of the form

$$\vec{S} = \hat{e}_x + \hat{e}_z \theta_0 \cos qx \tag{7}$$

Liquid crystals are known to have an anisotropic conductivity, $\sigma_\parallel > \sigma_\perp$.[11] Since the conductivity is anisotropic and the model director is generally not parallel to $\hat{e}_x$, the first application of an electric field in the z direction will lead to currents in both the z and the x directions. Since there is no source of current in the x direction, an electric field E_x must build up to oppose this current. It will have the form

$$E_x(x) = -\frac{(\sigma_\parallel - \sigma_\perp) \sin 2\theta \, E_z}{2(\sigma_\parallel \cos^2 \theta + \sigma_\perp \sin^2 \theta)} \underset{\theta_0 < \pi}{\propto} \theta_0 \cos qx \, E_z.$$

The origin of this field is similar to the origin of the Hall voltage with the exception that the anisotropy in the conductivity tensor is intrinsic to the liquid crystal and not produced by a magnetic field. The transverse field will be produced by space charge $\Sigma = \epsilon\epsilon_0(\partial E_x/\partial x)$ which is constant in sheets perpendicular to the x axis. The space charge will interact with the applied field to produce an electrostatic force ΣE_z. The electrostatic force is opposed by a viscous force. The steady state shear $\partial v_z/\partial x$ is such that

$$\frac{\partial v_z}{\partial x} = E_z^2 \frac{\epsilon_{\text{eff}}\epsilon_0}{\eta_{\text{eff}}} \frac{\sigma_\parallel - \sigma_\perp}{\sigma_\parallel \cos^2\theta + \sigma_\perp \sin^2\theta} \frac{\sin 2\theta}{2} \tag{8}$$

$$\frac{\partial v_z}{\partial x}_{\theta_0<\pi} \propto \theta_0 \cos qx \, E_z^2,$$

where v_z is the z component of the velocity and ϵ_{eff} and η_{eff} are the appropriate components of the dielectric constant and viscosity tensors respectively. Note that the shear is maximum where the director's tipping out of the x direction was assumed to be maximum. It is well known that shear can orient the director, in this case toward the z axis.[10] Thus there is a torque to twist the director to a larger amplitude distortion, producing more space charge. The possibility for instability is apparent. Helfrich has calculated that there will be a threshold voltage associated with this instability $V_t = V_c\, 2d/\lambda_t$. V_c is a voltage which is characteristic of the medium:

$$V_c = 2\pi \left[\frac{k_{33}\pi}{\frac{K_1\epsilon_\parallel}{\eta_1}\left(\frac{\epsilon_\perp}{\epsilon_\parallel} - \frac{\sigma_\perp}{\sigma_\parallel}\right) + (\epsilon_\parallel - \epsilon_\perp)\frac{\sigma_\perp}{\sigma_\parallel}} \right]^{1/2}, \tag{9}$$

where k_{33} is the " bend " elastic constant in the continuum theory of liquid crystals and K_1 is the constant giving the torque produced by a given amount of shear. Values for these constants for PAA can be found in the literature.[10] Since the anisotropy of the conductivity is known only approximately, the best possible theoretical value for V_c is 5 ± 1 V.

Helfrich's theory makes no definite prediction about λ_t and so it is not *a priori* possible to predict V_t. Experimentally it is found that $\lambda_t/2d \sim 0.7$. Figures 1 and 3 were drawn for square cells, $\lambda_t/2d = 1$ and for this particular case $V_c = V_t$. Thus both V_t and λ_t are neces-

sary to compare the experiment with Helfrich's theory. In order to predict λ_t a more complete boundary value analysis needs to be performed. The prediction for V_c is not temperature sensitive since η_1 and K_1 both vary as $(T)^{1/2}$; k_{33} and $(\sigma_\parallel - \sigma_\perp)/\sigma_\parallel$ both decrease with increasing temperature.

The trial function for $\vec{S}$ used by Helfrich, Eq. (7), does not allow for boundary conditions $\vec{S} = \hat{e}_x$ at $z = \pm d/2$. The drumhead distribution of Eq. (1) is a straightforward extension of Helfrich's original assumption, Eq. (7). The basic equations in Helfrich's theory are altered only by a small amount of splay restoring force, measured by k_{11}. The conclusions are unaffected. We now show that this slight extension of the theory is in one to one correspondence with the experimental results. (1) The predicted characteristic voltage of 5 ± 1 V is in quantitative agreement with the normalized experimental threshold voltage of 5.5 ± 0.2 V. Neither the experimental or theoretical voltages are temperature sensitive. (2) The domain pattern should be visible only for light polarized parallel to the x direction since the instability is predicted to take place only in the x–z plane. This has also been observed.[6,7,13,25,26] (3) The regions of maximum tipping angle are predicted to be areas of maximum shear; as can be seen by comparing Eqs. (7) and (8). This is the experimental observation as can be seen from a comparison of Figs. 1 and 3. (4) The characteristic frequency in this model should be the space charge relaxation frequency. The torque produced by the electrostatic interaction is independent of the direction of E_z. The model does not require the relatively long times for build-up of a SCL distribution of Eq. (4). The $(RC)^{-1}$ relaxation frequency has been observed. (5) The relative insensitivity of V_t to the sample conductivity can be understood by reference to Eq. (9). The conductivity enters the equation as a ratio $\sigma_\perp/\sigma_\parallel$. Thus the anisotropy of the conductivity is the important quantity, not the carrier density. Since the anisotropy of the conductivity is a property of the liquid crystal, the experiment does not depend on the details of the impurity ion conduction. In fact the domain experiment has nothing to contribute concerning the nature of the conduction. (6) The space charge generation arises in this model from a separation of intrinsic ionic charges and does not require injection. Thus the mechanism will work with purely capacitive coupling, which is the experimental

observation. (7) The model does not necessarily rule out fluid motion in the isotropic phase. If one assumes that $\epsilon_\parallel = \epsilon_\perp$, Eq. (9) shows that V_c^2 is proportional to $k_{33}\sigma_\parallel/(\sigma_\parallel - \sigma_\perp)$. As the temperature rises to the nematic–isotropic transition in zero electric field, both the numerator and the denominator go to zero. The resultant value is undetermined. It is also known that an electric field can induce order in the isotropic phase.[27] Thus k_{33} and $(\sigma_\parallel - \sigma_\perp)/\sigma_\parallel$ may not be zero in the isotropic phase in an electric field. More work will be necessary to determine what is to be expected from Helfrich's model in the isotropic phase having electric field induced order.

The electric field induced domain patterns in nematic liquid crystals bear a certain resemblance to the heat convection patterns of Bénard.[28] Rough estimates of the physical parameters predict that a thermal convection instability would be possible only for thicknesses greater than 1 mm. Indeed the Bénard instability has been observed by Naggiar[29] with samples of this thickness. Naggiar also observed the electric field induced patterns, thus clearly distinguishing between the thermal and space charge mechanisms. For the experiments described here, thermal instability cannot play a significant role.

6. Conclusion

We believe that the excellent agreement between the experiments with the AC driven domains and Helfrich's theory constitute a proof of the conduction induced torque mechanism. While a unipolar space charge injection mechanism may have a role in the DC fluid motion in both the liquid crystal and isotropic phases, it has been shown that this mechanism cannot be dominant in AC driven samples of moderate conductivity. Unfortunately the DC experiments and theories are much more difficult to interpret due to the complicated problem of charge transfer at the liquid–solid interfaces. It is encouraging, however, to be able to understand the electrohydrodynamic mode which is unique to the liquid crystal phase.

Acknowledgements

The author wishes to acknowledge many stimulating and fruitful discussions with Dr. T. K. Hunt.

Appendix: A Brief Historical Review

Current work is beginning to clear up a long standing problem in liquid crystals: the influence of electric fields in nematics. During the 1920s and 30s, considerable work was done in this area. People were interested in electric susceptibilities (dielectric constants) in order to determine the molecular orientation. Unfortunately the early results were often contradictory. In his book, Gray writes, " The general position of the literature in relation to the direction of the long molecular axis is, however, extremely confusing. A great deal of work has been carried out by different authors, and the conclusions are frequently conflicting ".[30] Some of the workers were Friedel,[31] Zocher and Birstein,[32] Ornstein and Kast,[33] Frederiks and Tzvetkov,[34] Herman, Krunmacher and May,[35] and Naggiar.[29] Generally their experiments were designed to measure the orientation of the molecules as a result of a dielectric interaction. As several authors have shown recently, the response of the liquid crystal to electric fields is due to electric current and mass flow. In fact several early authors speculated that a current induced hydrodynamic phenomenon was involved. Frederiks and Zolina[4] actually observed that dust was set in motion above a certain electric field. It appears, however, that no one was sufficiently interested in the problem to carry through the necessary theoretical analysis. A second reason for the early confusion about the problem is that transparent electrodes were not generally available in the 1930s. Thus the early experiments were performed in geometries that did not lend themselves to interpretation, and that did not yield the striking optical switching phenomena. It seems to be clear from the literature, however, that optical patterns have been identified as being induced by electric fields in the early 1930s.

REFERENCES

1. Heilmeier, G. H., Zanoni, L. A. and Barton, L. A., *Proc. IEEE* **56**, 1152 (1968).
2. Williams, R., *J. Chem. Phys.* **39**, 384 (1963).
3. Kosterin, E. A. and Chistyakov, I. G., *Kristalografuja* **13**, 295 (1968) [*Sov. Phys.-Crystallogr.* **13**, 229 (1968)].
4. Freederick, V. and Zolina, V., *Trans. Faraday Soc.* **29**, 919 (1933).
5. *Final Report of University of Cincinnati to U.S. Air Force*, Contract A.F. 33(616)–33, July 1 (1955).

c

6. Durand, G., Veyasie, M., Rondelez, F. and Léger, L., C. R. *Acad. Sc. Paris* **270B,** 97 (1970).
7. Penz. P. A., *Phys. Rev. Letters* **24,** 1405 (1970); **25,** 489 (1970).
8. Koelmans, H. and van Boxtel, A. M., *Phys. Letters* **32A,** 32 (1970).
9. See also several papers presented at the *Third International Liquid Crystal Conference* and included in the proceedings published in current issues of this journal.
10. Helfrich, W., *J. Chem. Phys.* **51,** 4092 (1969).
11. Chatelain, P., *Acta Cryst.* **1,** 315 (1948).
12. Chatelain, P., *Bull. Soc. Franc. Mineral. Crist.* **60,** 280 (1937).
13. Teaney, D. T. and Migliori, A., *J. Appl. Phys.* **41,** 998 (1970).
14. Assouline, G. and Leiba, E., *J. Phys.* (*Paris*) **30,** C4–109 (1969).
15. Penz, P. A., *Bull. Am. Phys. Soc.* **15,** 59 (1970).
16. Twitchell, R. P. and Carr, E. F., *J. Chem. Phys.* **46,** 2765 (1967).
17. Maier, W. and Meier, G., *Z. Naturforsch.* **16a,** 470 (1961).
18. Felici, N., *Rev. Gen. Elect.* **78,** 717 (1969).
19. Schneider, J. M. and Watson, P. K., *Phys. of Fluids* **13,** 1948 (1970).
20. Watson, P. K., Schneider, J. M. and Till, H. R., *Phys. of Fluids* **13,** 1955 (1970).
21. Miesowicz, M., *Nature* **158,** 27 (1946).
22. Lampert, M. A., and Mark, P., *Current Injection in Solids*, Academic Press, New York, 1970, 18.
23. Blinc, R. *et al.*, *Phys. Rev. Letters* **23,** 969 (1970).
24. Carr, E. F., *Ordered Fluids and Liquid Crystals*, edited by Porter, R. S. and Johnson, J. F., Advances in Chemistry Series 63, Washington, D.C. 1967, 76.
25. Helfrich, W., *J. Chem. Phys.* **51,** 2755 (1969).
26. Deutsch, Ch. and Keating, P. N., *J. App. Phys.* **40,** 4049 (1969).
27. Eisenmann, J. Zodac-Kahn, *Ann. Phys.* (*Paris*) **6,** 455 (1936).
28. Chandrasekhar, S., *Hydrodynamic and Hydromagnetic Stability*, Clarendon Press, Oxford, 1961, 10.
29. Naggiar, V., *Ann. Phys.* (*Paris*) **18,** 5 (1943).
30. Gray, G. W., *Molecular Structure and the Properties of Liquid Crystals*, Academic Press Inc., New York, 1962, 74.
31. Freidel, G., *Ann. Phys.* (*Paris*) **18,** 273 (1922).
32. Zocher, H. and Birstein, V., *Z. Physik. Chemie* **A142,** 186 (1929).
33. Ornstein, L. S. and Kast, W., *Trans. Faraday Soc.* **29,** 931 (1933).
34. Zvetkov, V. N., *Acta Physiochim. URSS* **6,** 865 (1937).
35. Hermann, K., Krummacher, A. H. and May, K., *Z. Phys.* **73,** 419 (1931).